Supporting Information for "Relative roles of plume and coastal forcing on exchange flow variability of a glacial fjord"

Robert Sanchez[1], Fiammetta Straneo[1], Kenneth Hughes[2], Philip Barbour[2],

Emily Shroyer[2,3]

[1]Scripps Institution of Oceanography, UC San Diego, San Diego, CA, USA

[2]College of Earth, Ocean, and Atmospheric Sciences, Oregon State University, Corvallis, OR, USA

[3]Office of Naval Research

Contents of this file

1. Text S1 to S3

2. Figures S1 to S9

3. Tables S1

Text S1. Comparison against Profiles.

We compare the model output to CTD profiles collected in August 2015 and July 2017 and categorize the profiles as shelf (N=24) and fjord (N=48) profiles. Figure 2 of the main text shows all the profiles collected in summer. When all profiles are averaged together, we see the model (solid, Fig. S1a) does a reasonable job of capturing the observed (dashed, Fig S1a) mean temperature at depth. However, this mean is expected to be captured because the ASTE boundary conditions were shifted to be in line with the observations

at 350 m. It also recreates the basic vertical structure of temperature with a warm AW mass at depth, a cold PW mass around 100 m, and a WPW mass near the surface. We also include the average of XCTD profiles taken in March 2010 and compare it to the mean model output at SF4 in March 2016. The winter profiles are from a different year and so a direct comparison is limited, but the model pycnocline appears significantly shallower than in observations and is generally saltier. Unfortunately, in all seasons, the model overestimates the temperature of the PW resulting in a warm bias. Reasons for this bias potentially include the lack of icebergs in the fjord, lack of sea ice along the coast and a warm bias from the ASTE boundary conditions. The model also overestimates the salinity above 300 m resulting in weaker stratification in the model than in reality (Fig. S1b). In both the temperature and salinity fields, the differences between the model and observations are much larger than the differences between the fjord and the shelf.

Velocity and volume transport from the model are compared to ADCP data from the middle of fjord (SF4) and the shelf (OW1). At SF4, we break the velocity record into a summer (June 1 – August 31) and winter (October 1 – May 1) time series similar to Jackson and Straneo (2016). The seasonal mean (from two years) along-fjord velocity structure from the observations compares poorly to the model output (Sup. Fig. S1c,d) due to the challenges in recreating realistic fjord stratification. During the summer, the model outflow is at the surface while the observations show outlfow centered around 100 m. This mismatch can largely be explained by plume dynamics as the model stratification is much weaker than the observations (Sup. Fig. S1b) resulting in a plume that reaches close to the surface rather than finding a deeper neutral buoyancy (De Andrés et al., 2020). The primary inflow which compensates the outflow is therefore also shallower in the model.

Kajanto, Straneo, and Nisancioglu (2022) showed that with icebergs the stratification increased and the plume was deeper. Additionally, iceberg drag might contribute to a deeper neutral buoyancy depth. In the winter, the profiles also have a mismatch that can potentially be explained by fjord stratification. In the observations, the fjord has a sharp pycnocline around 200 m (sup. Fig. S1b) while the model lacks this pycnocline. This difference in pycnocline structure and depth results in a concentrated baroclinic flow centered around 200 m in the observations and a diffuse baroclinic flow centered closer to 350 m in the model.

Text S2. ADCP Transport.

We estimate volume transport from the ADCP using 3 methods of extrapolation: surface extrapolation using constant shear from the top three bins, surface extrapolation using a constant value, and bottom extrapolation using a linear shear down to zero (Jackson & Straneo, 2016). For each method, the part of the water column not extrapolated is filled with a constant value to ensure no net transport. We multiply this velocity profile by the fjord width and use two different estimates of fjord width resulting in 6 transport estimates that we use to define uncertainty. We apply a 30-day rolling mean to velocities prior to calculating incoming volume transport. The ADCP-derived incoming volume transport is the same magnitude as the modeled transport, but has a larger volume flux during the summer than the model and a smaller flux in the winter (Sup. Fig. S2). While the instantaneous velocities in the winter can be much higher than in the summer, averaging removes most of the oscillatory signal resulting in weaker average velocities (Sup. Fig. S1).

We also compare the 30-day rolling mean model velocity in the western end of Sermilik Trough with the 30-day rolling mean velocity recorded at OW1 focusing on the depth 120 m where data was cleanest (Sup. Fig. S2). The along-shelf modeled velocity was significantly larger than the observed velocity reaching velocities around 0.3 m/s in the model compared to 0.1 m/s by the ADCP. However, both are flowing westward with a mean negative velocity, consistent with the presence of an equatorward coastal current, and both are minimized in the summer when winds and coastal current freshening are weakest. It could be that the disagreement is poor because the mooring with the ADCP is located on a slightly different part of the shelf than where we sample in the model. Additionally, if we are not recreating the position of the coastal current correctly it could result in a large difference between the observed and modeled velocity.

Text S3. Discussion of CTW parameters.

A majority of the parameters used in the CTW Eq. 3 of the main text are straightforward to determine, but the baroclinic wave speed c and the pycnocline amplitude η both require user discretion. c is calculated as the zero-crossing of the first normal mode using density profiles from the mouth of the fjord, but it varies across the mouth by ± 0.15 m/s and the depth of the of the pycnocline can vary as well between ± 60 m at a single timestep. We use cross-section averages to determine c as most of this variability is due to differences in fjord depth which can lower the pycnocline height.

We used two different methods to determine η. The first was simply to the take the depth of the pycnocline determined from the normal-mode analysis and then remove the mean. The second method, described in the main text, used the cross-section average density fluctuations divided by the stratification. Both methods produced similar ampli-

tudes on timescales longer than 15-days (Fig. S8), but the method based on stratification produced a larger response on shorter timescales. We believe the normal-mode method, while useful for determining the pycnocline depth, might underestimate pycnocline fluctuations on shorter timescales since it responds to rapid changes in density structure by finding a new zero crossing rather than tracking the previous pycnocline as it fluctuates.

We evaluate how much CTWs contribute to the high-frequency variability by comparing the estimate from CTW theory against a 15-day high-pass filter of incoming volume flux (Fig. S9). The seasonality of the two volume fluxes are consistent with peaks in winter months and are a similar magnitude. However, there is still substantial higher-frequency variability in the summer in the model and we cannot attribute much of this to CTWs. The standard deviation of the model is 46 mSv and of the theory is 30 mSv. Therefore, we can say that CTW theory is either underestimating the magnitude of the circulation or additional high-frequency variability is a significant component of the incoming volume flux. Model animations (not shown) suggest eddies could potentially play a role.

References

De Andrés, E., Slater, D. A., Straneo, F., Otero, J., Das, S., & Navarro, F. (2020). Surface emergence of glacial plumes determined by fjord stratification. *Cryosphere Discuss.*, 1–41. doi: 10.5194/tc-2019-264

Jackson, R. H., & Straneo, F. (2016). Heat, Salt, and Freshwater Budgets for a Glacial Fjord in Greenland. *J. Phys. Oceanogr.*, *46*, 2735–2768. doi: 10.1175/JPO-D-15-0134.1

Kajanto, K., Straneo, F., & Nisancioglu, K. (2022). Impact of icebergs on the seasonal submarine melt of Sermeq Kujalleq. *The Cryosphere Discuss.*, 1-26. doi: 10.5194/tc-2022-136

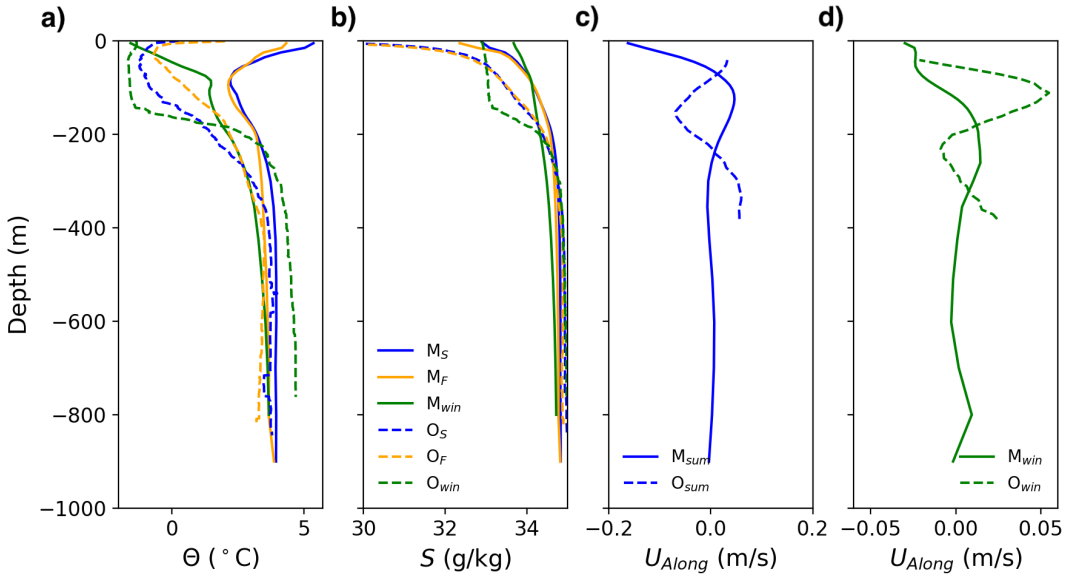

Figure S1. Profile comparison of model and observations. a) the spatially-averaged CTD temperature profiles versus depth for both the model (solid) and observations (dashed) in the fjord (yellow, N=48), on the shelf (blue, N=24), and in the winter (green, N=4). b) same but for absolute salinity. c) The average along-fjord velocity at SF4 during the summer (June 1 – August 31). The solid line is the model and the dashed line comes from the SF4 ADCP. d) same as c but for the winter (October 1 – May 1.)

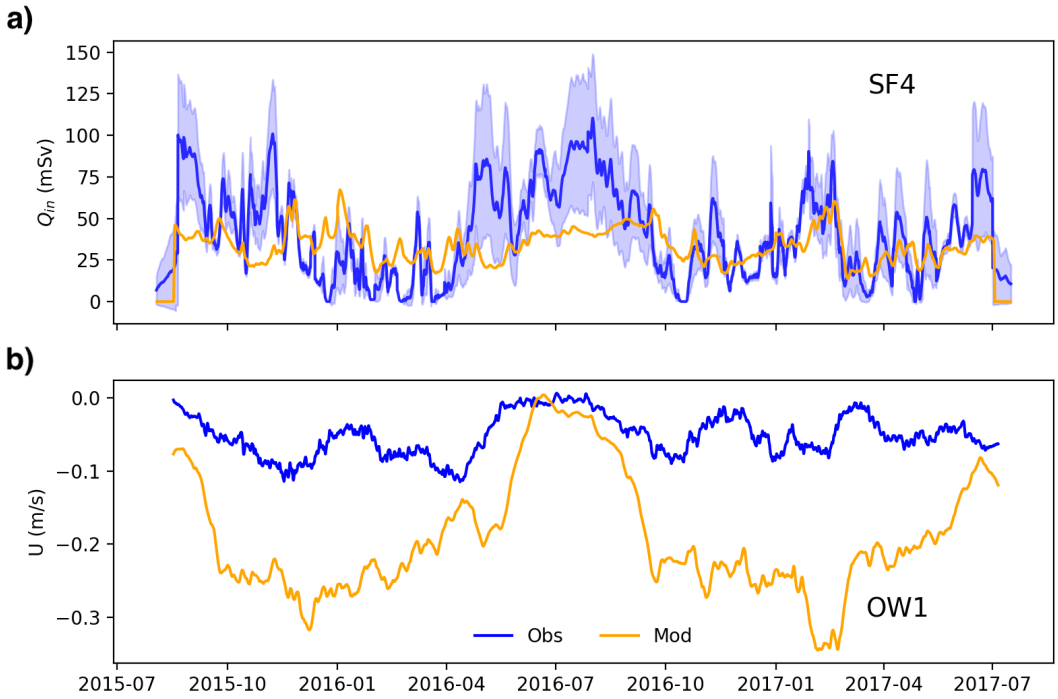

Figure S2. Velocity comparison of model and observations. a) The incoming volume transport calculated from the ADCP at SF4 (blue) and model output (orange). b) The along-shelf velocity averaged over 110 – 130 m from the ADCP at SF6 and the model. All velocities have had a 30-day rolling mean applied.

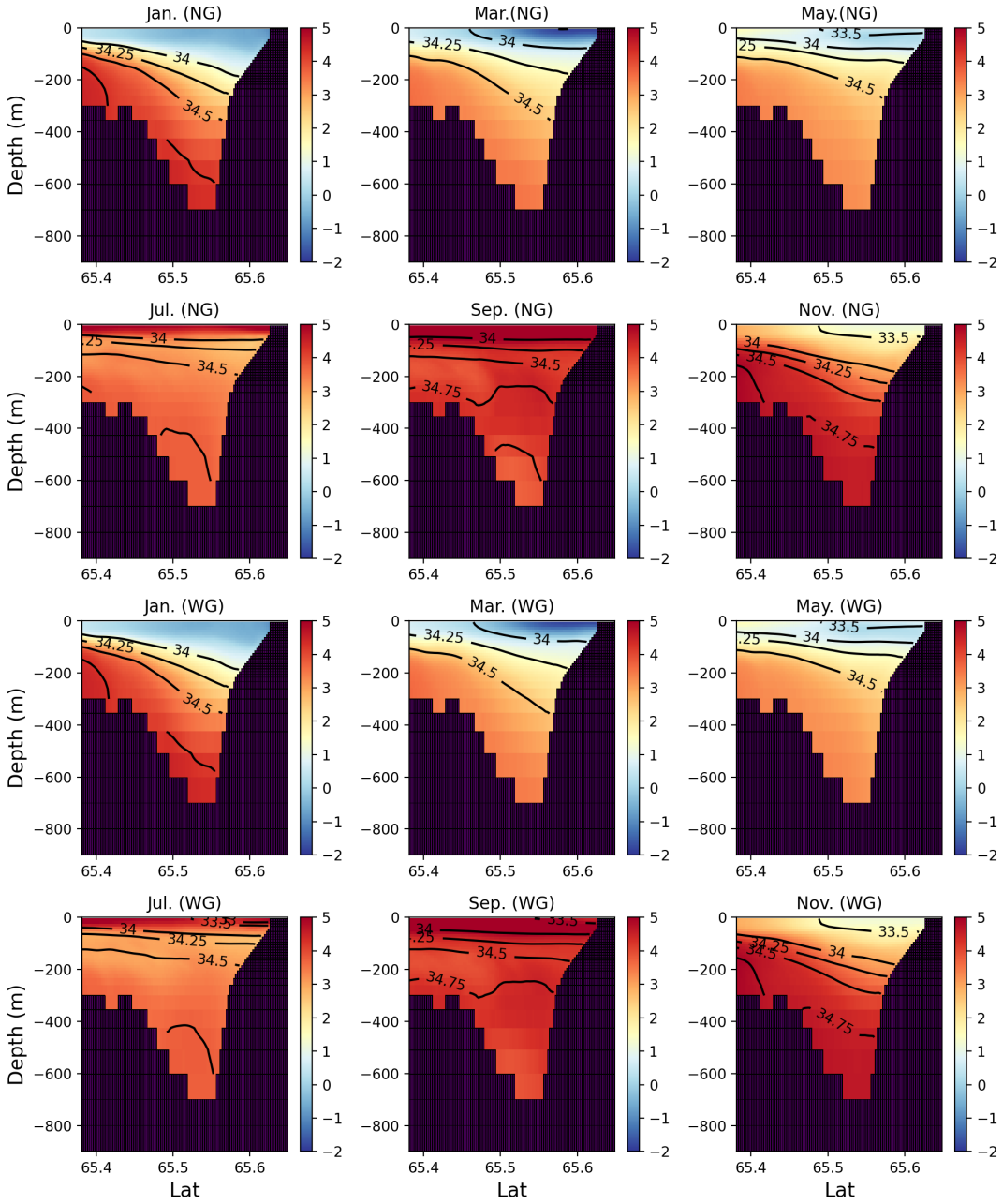

Figure S3. Monthly-average shelf temperature transect downstream (west) of the fjord. Contours are isohalines (32,32.5,33,33.5,34,34.25, 34.5,34.75,35) g/kg. The top six panels are from the NG run, the bottom six are from the WG run.

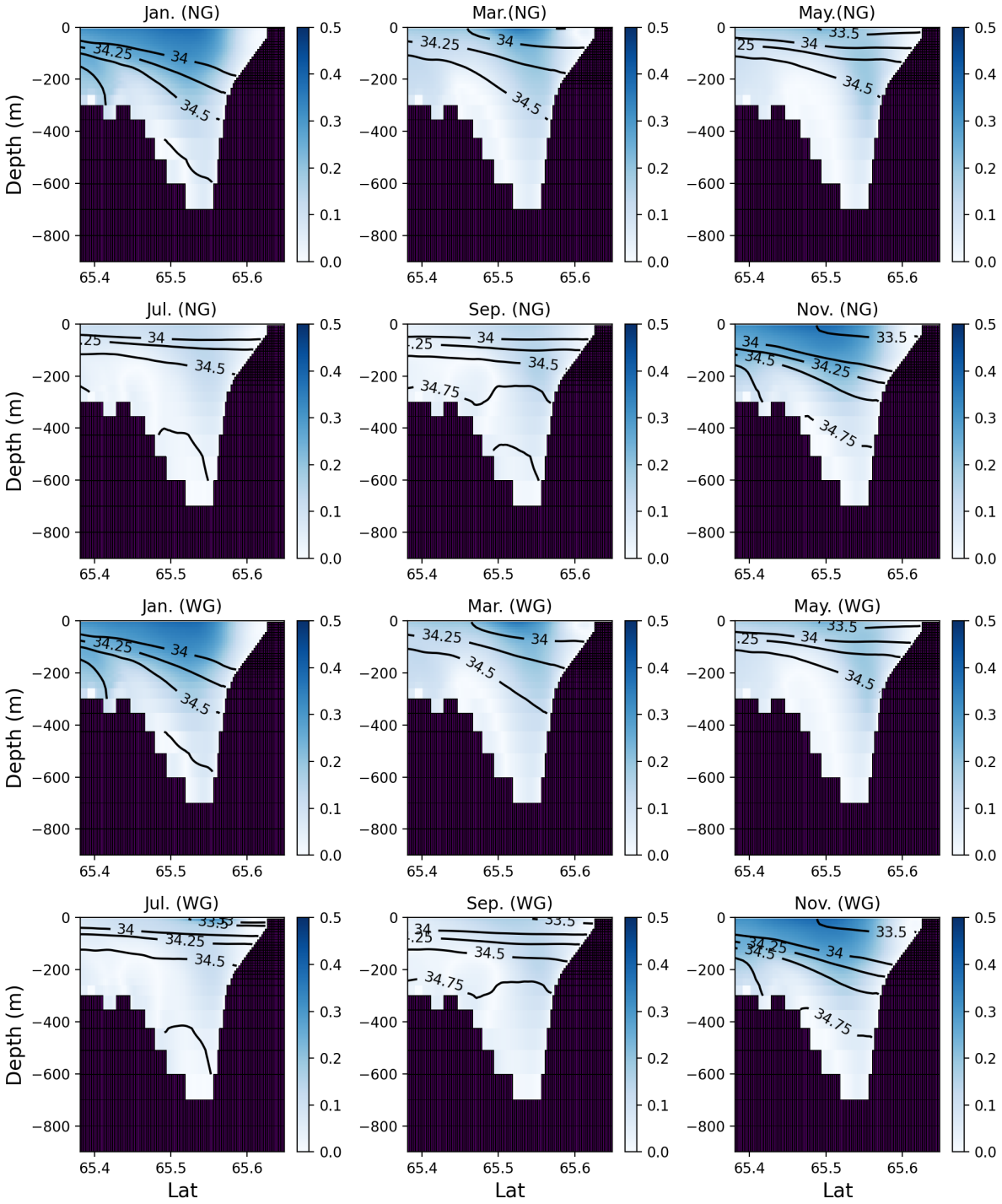

Figure S4. Monthly-average shelf velocity transect downstream (west) of the fjord. Positive velocity is oriented west. Contours are isohalines (32,32.5,33,33.5,34,34.25, 34.5,34.75,35) g/kg. The top six panels are from the NG run, the bottom six are from the WG run.

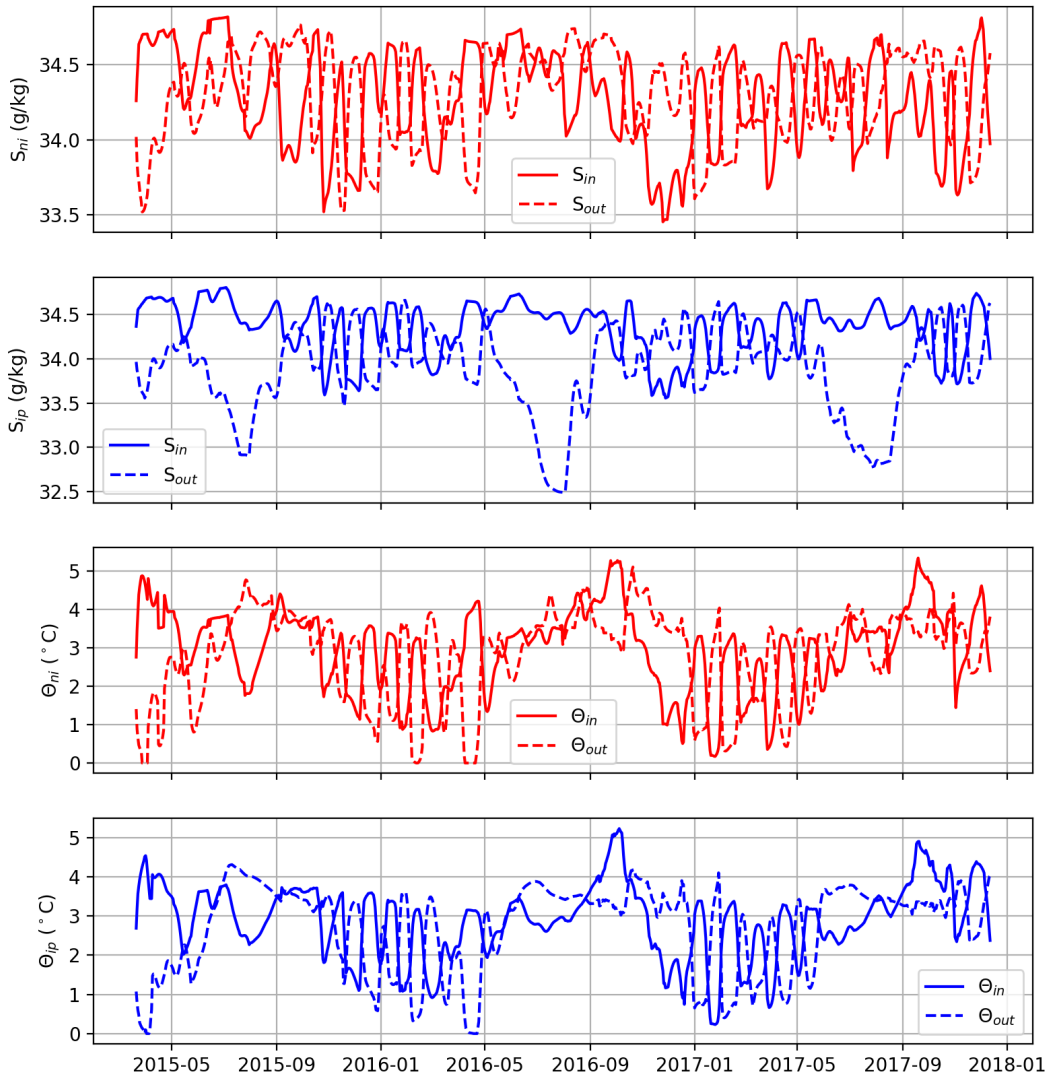

Figure S5. Additional Time Series of TEF bulk values. a) The TEF Salinity time series for the NG run. b) The TEF Salinity time series for the WG run. c) The TEF temperature time series for the NG Run. d) The TEF temperature series for the WG run. These values were used in the calculation of ΔS and $\Delta\Theta$ in Fig. 14 main text

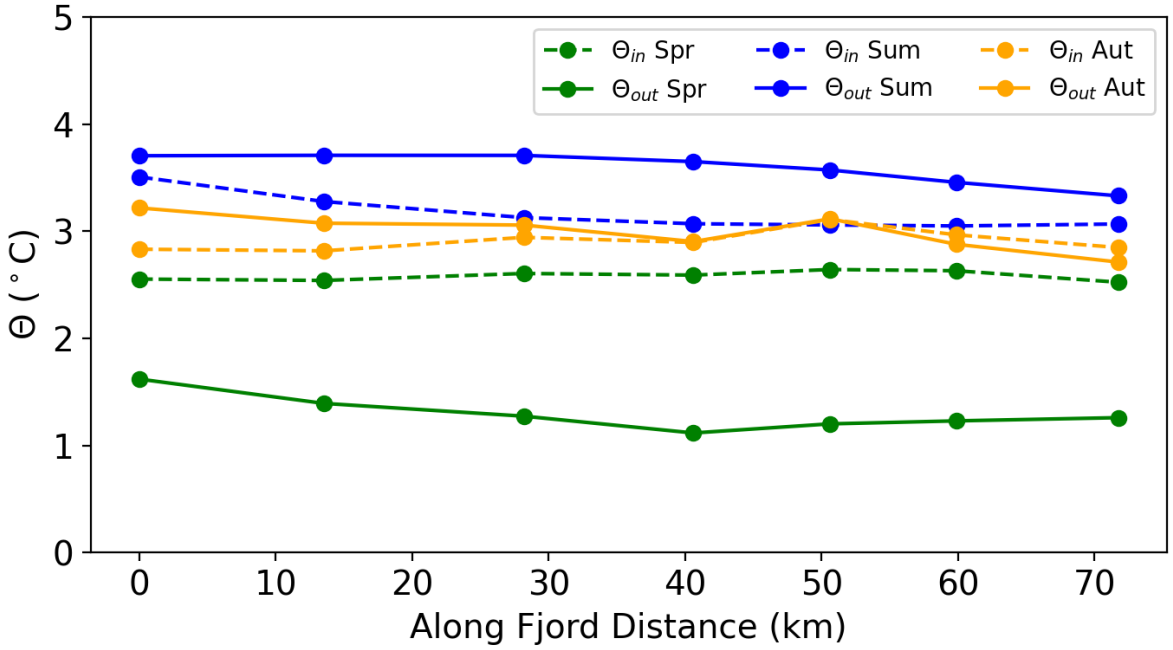

Figure S6. TEF along fjord Θ_{in}. Seasons are three month averages. The x-axis is distance from the mouth. Compare to Fig. 15 main text

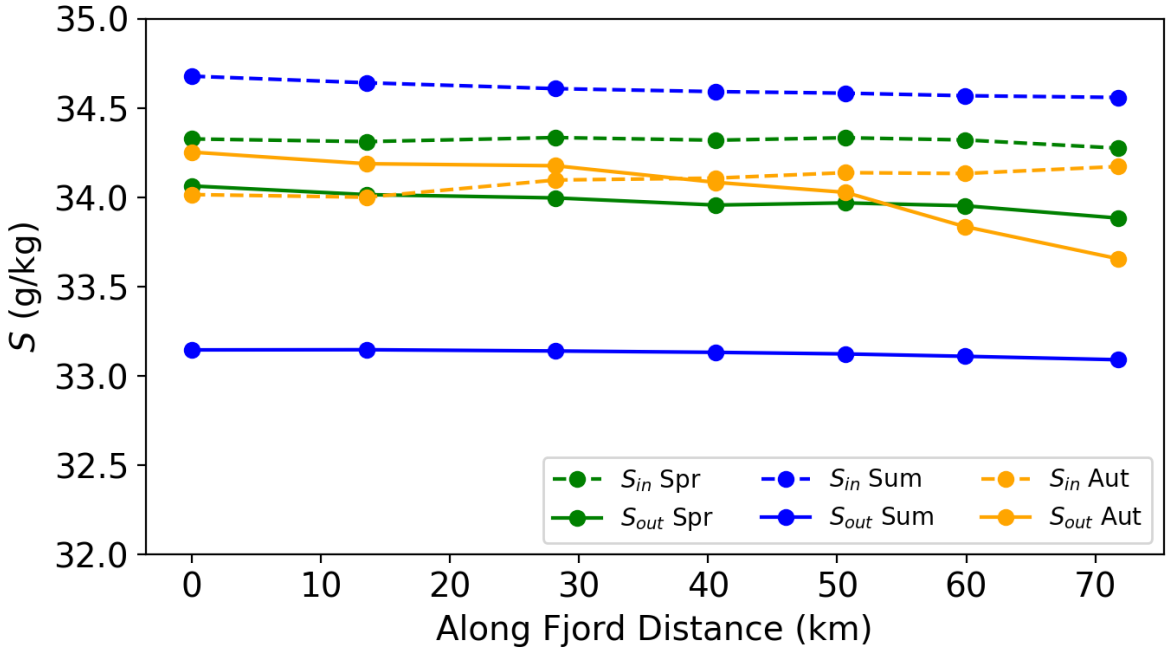

Figure S7. TEF along fjord S_{in}. Seasons are three month averages. The x-axis is distance from the mouth. Compare to Fig. 15 main text

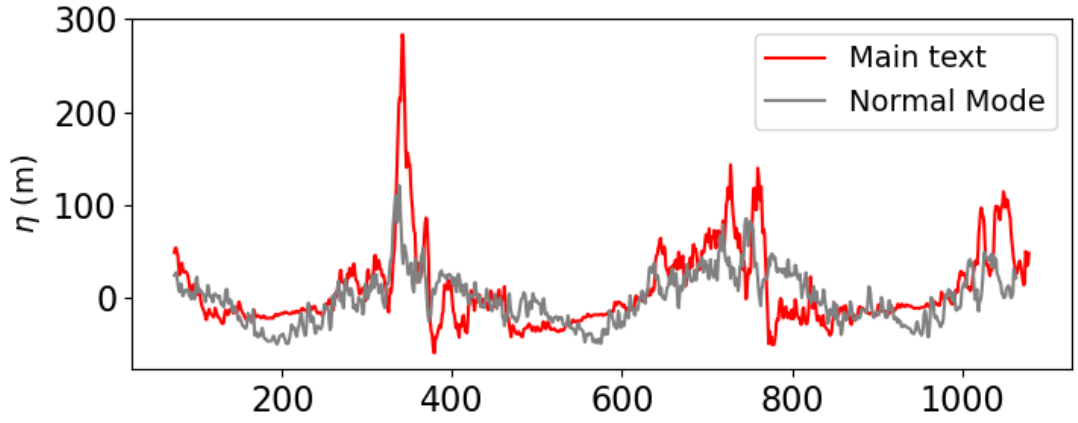

Figure S8. Comparison of the pycnocline amplitude based on different methods. The pycnocline amplitude based on the normal mode method (gray) and the method used in the main text (red). The main text method is the density anomaly divided by the mean stratification.

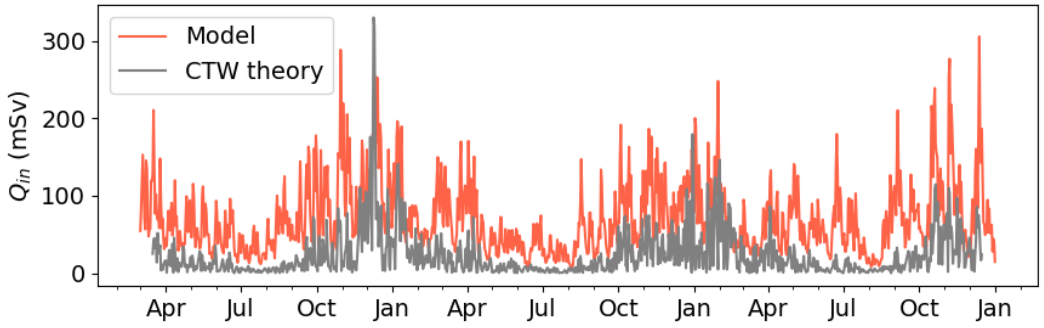

Figure S9. Incoming volume flux comparison against theory. The incoming volume flux from the model (red) and the predicted flux from CTW theory (gray). The incoming flux has been high-pass filtered to 15 days.

Table S1. Statistics and skill scores for the summer CTD data. The first column is the variable and includes the model skill in vertically-averaged salinity and temperature ($\overline{S}, \overline{\Theta}$), and the skill for the model and observations for the vertical stratification (N_S, N_Θ). Significance is denoted with a star. A skill score < 0.2 is considered poor.

Variable	SS	MSE	r
$\overline{S}$	0.26	0.49	0.97*
$\overline{\Theta}$	< 0	4.1	-0.13
N_S	< 0	0.93	0.65*
N_Θ	< 0	11.23	-0.08